Available online at www.sciencedirect.com

ScienceDirect

Physics Procedia 70 (2015) 945 – 948

Physics Procedia

2015 International Congress on Ultrasonics, 2015 ICU Metz

Guided wave generation in elastic layered substrates with piezoelectric coatings and patches

E.V. Glushkov[a,*], N.V. Glushkova[a], A.A. Evdokimov[a], Ch. Zhang[b]

[a]*Kuban State University, IMMI, Stavropolskaya str., 149, 350040 Krasnodar, Russia*

[b]*bUniversity of Siegen, Department of Civil Engineering, Paul-Bonatz-Str. 9-11, 57076 Siegen, Germany*

Abstract

Piezoelectrically generated surface and pseudosurface acoustic waves are simulated and analyzed in the mathematical framework based on the integral representations and guided wave asymptotics. In addition to the abilities of the conventional modal analysis, the integral equation approach explicitly provides the amplitudes of waves generated by a specified source, making it possible to evaluate the wave energy transmitted from the source into the substrate and its distribution among the excited guided waves. Diamond based microdevices and piezoelectric patch actuators are considered as examples.

Peer-review under responsibility of the Scientific Committee of ICU 2015

Keywords: SAW devices; piezoelectric active sensor array; integral equation based simulation; piezopatch-structure contact problem

1. Introduction

The action of many microdevices is based on the guided acoustic wave generation and propagation in elastic substrates. The guided wave (GW) characteristics required for the evaluation and optimization of their performance are obtained on the basis of mathematical and computer modeling. A conventional tool of GW study is the modal analysis technique yielding the wavenumber, velocity and spatial eigenform of every GW mode supported by the waveguide structure considered. However, since every eigensolution is defined up to a constant factor, the modal analysis cannot directly provide the amplitude and energy characteristics of the GWs generated by a specified source. Hence, it is not possible to evaluate such important characteristics for the device design as the total amount of wave energy supplied by a driving electric signal at a certain central frequency and its distribution among the excited GWs. Such a study assumes the use of coupled source-structure solutions of non-homogeneous boundary value problems (BVP), in which the source action is accounted for via non-zero boundary conditions. At present, this kind of work is mostly executed using commercial FEM packages that can provide quantitative data with practically arbitrary geometry and material properties of simulated objects. However, their use is often computationally expensive, not giving direct information on the GW characteristics.

* Corresponding author

E-mail address: evg@math.kubsu.ru

Peer-review under responsibility of the Scientific Committee of ICU 2015

doi:10.1016/j.phpro.2015.08.196

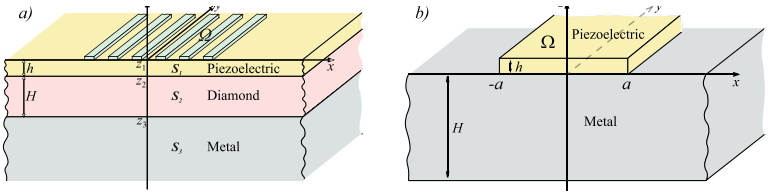

Fig. 1. Geometry of the problems: (a) diamond-based device; (b) PWAS.

At the same time, there exists a way to obtain the same physically evident and low-cost GW representations as the modal analysis provides but, in addition, uniquely fixing the amplitude (and so the energy) of every excited wave depending on the source and structural parameters. This approach is based on the integral transform application to BVPs simulating waveguide structures with plane-parallel boundaries. It allows one to derive an explicit BVP solution in the form of inverse Fourier-transform path integrals. The residual technique reduces it then to the form of GW expansion, e.g., in the 2D case:

$$\mathbf{v}(x,z)e^{-i\omega t} = \frac{1}{2\pi}\int_{\Gamma}\mathbf{V}(\alpha,z)e^{-i(\alpha x+\omega t)}d\alpha \sim \sum_{n}\mathbf{a}_n(z)e^{i(\zeta_n x-\omega t)}, \quad x > a. \tag{1}$$

Here $\mathbf{v} = (\mathbf{u},\varphi)$ is the complex amplitude of a coupled elastoelectric time-harmonic field, $\mathbf{V} = \mathcal{F}_x[\mathbf{v}]$ is its Fourier-transform symbol with respect to the horizontal variable x, and $\mathbf{a}_n = -i\,\mathrm{res}\,\mathbf{V}|_{\alpha=-\zeta_n}$, where ζ_n are all real poles of the integrand $\mathbf{V}$ plus a finite number of the nearest complex ones to the real axis; $\omega = 2\pi f$ is angular frequency. The poles enter in the expansion as wavenumbers, yielding constant traveling waves with real ζ_n (surface acoustic waves – SAW) and decaying ones with complex ζ_n (pseudosurface acoustic waves - PSAW). The phase velocity c_n, wavelength λ_n, and logarithmic decrement δ_n of every GW specified by the summands in Eq. (1) are $c_n = \omega/\mathrm{Re}\,\zeta_n$, $\lambda_n = 2\pi/\mathrm{Re}\,\zeta_n$, and $\delta_n = 2\pi\,\mathrm{Im}\,\zeta_n/\mathrm{Re}\,\zeta_n$.

The solution in the Fourier transform domain can be derived in terms of the Fourier symbols of the Green's matrix of the structure $k(\mathbf{x})$ and the source vector $\mathbf{q}(x)$:

$$\mathbf{V}(\alpha,z) = K(\alpha,z)\mathbf{Q}(\alpha), \quad K = \mathcal{F}_x[k] \quad \text{and} \quad \mathbf{Q} = \mathcal{F}_x[\mathbf{q}]. \tag{2}$$

Thus, the amplitude vectors $\mathbf{a}_n$ defined by the residues uniquely account for the spatial GW eigenforms (z-dependencies) via Green's matrix and for the source characteristics via $\mathbf{Q}(\zeta_n)$.

The abilities of the integral equation approach are demonstrated with two examples of its implementation: 1) for SAW microdevices fabricated from polycrystalline diamond layers covered by piezoelectric films (Fig. 1a) and 2) for piezoelectric wafer active sensors (PWAS) used for guided wave generation and registration in structural health monitoring (SHM) systems (Fig. 1b).

2. Diamond based SAW devices

Polycrystalline diamond layers are attractive substrates for SAW devices because the diamond provides the highest wave velocity among all other materials; Nakahata et al. (1995); Benetti et al. (2005). To enable piezoelectric SAW excitation, a non-piezoelectric diamond layer is covered with a thin piezoelectric coating (Fig. 1a). Among those, ZnO and AlN also provide high acoustic wave velocity; Benetti et al. (2005); Wu et al. (2008). The mathematical framework and detailed description of the integral equation based models developed for such structures can be found in Glushkov et al. (2012). That work was focused on the effect of PSAW-to-SAW degeneration at certain discrete values h/λ (h is the thickness of the piezoelectric film and λ is the GW wavelength). The use of such degenerating PSAWs with low leakage losses looks advantageous because they possess higher phase velocities than SAWs. Earlier, the optimal ratios h/λ were discovered and experimentally verified for the first pseudo-surface (Sezawa) mode in the two-layer AlN/Diamond structure ($N = 2$, $H = \infty$); Benetti et al. (2005). The research of Glushkov et al. (2012) has revealed this effect for higher modes as well as examined its manifestation in three-layer structures with different diamond-to-AlN thickness ratio H/h. A finite thickness of the diamond layer ($N = 3$, $H < \infty$) results in more complicated dispersion curve patterns than in the two-layer case (Fig. 2).

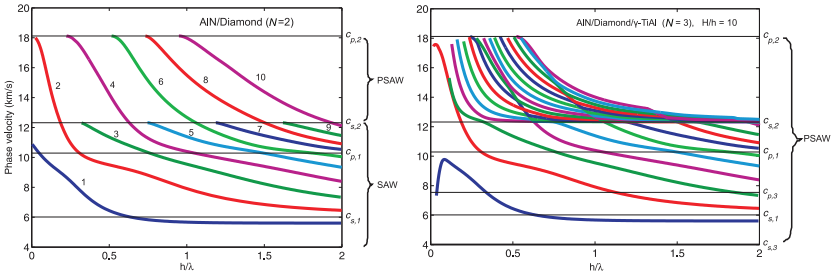

Fig. 2. SAW-PSAW phase velocities in (a) two- and (b) three-layer structures.

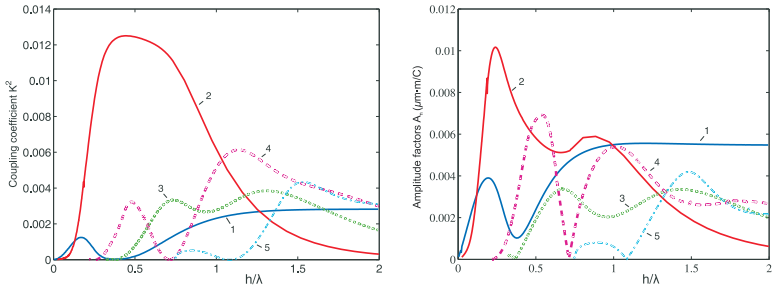

Fig. 3. (a) Coupling coefficients, (b) GW amplitudes.

The ranges of SAW and PSAW in Fig. 2 are differentiated by the velocity c_s of the bulk S-waves in the underlying elastic half-space. In the two-layer structure, the threshold is determined by a rather high S-wave velocity in the diamond: $c_s = c_{s,2} = 12.32$ km/s. The phase velocity curves beneath this level ($c_n < c_s$) are for the undamped SAWs while those above this boundary ($c_n > c_s$) are real parts of the complex PSAWs' phase velocities ω/ζ_n. The wavenumber $\kappa_s = \omega/c_s$ is a branch point of the Fourier domain solution $\mathbf{V}(\alpha, z)$, and the SAW real poles ζ_n come out from the real axis into the complex α-plane when pass through $\alpha = \kappa_s$ if tracing them from right to left. The even ones get on the physical Riemann surface sheet while the odd ones go off onto the unphysical sheet ceasing contribution into the GW expansion in Eq. (1). Consequently, they are not drawn above c_s in Fig. 2a.

In the $N = 3$ case, the threshold velocity c_s in the lower metallic γ-TiAl half-space is considerably less than that in the diamond: $c_s = c_{s,3} = 4.04$ km/s. It implies that all former real (SAW) branches shown in Fig. 2a become formally complex in the three-layer model (Fig. 2b). Nevertheless, with a sufficiently large ratio H/h, the pattern of former real dispersion curves changes insignificantly and their losses δ_n are also negligible. Above the former threshold $c_{s,2}$, the loss decrements δ_n increase. However, the effect of PSAW-to-SAW degeneration still remains, manifesting itself in sharp δ_n decreases at certain h/λ. Since $c_{s,2}$ is no longer a branch point, all the curves passing this level remain in the physical sheet. The curves above $c_{s,2}$ are sharply shifted to the left that makes their presence in this range much denser compared to Fig. 2a.

Conventionally, the structure's ability to produce various GWs in response to an applied voltage is estimated via the coupling coefficients $K_n^2 = 2(c_n^o - c_n^s)/c_n^o$, where c_n^o and c_n^s are phase velocities of the nth GW mode propagating over open-circuited and short-circuited surfaces, respectively. Figure 3a depicts K^2 versus h/λ for the first five SAW modes shown in Fig. 2a. Their pattern coincides with that presented in Wu et al. (2008). It is interesting to compare the K^2 dependences with the relative amplitude factors $A_n = |\mathbf{a}_n(0)/d|$ shown in Fig. 3b. Here $\mathbf{a}_n$ are the displacement vector-coefficients in GW expansion (1) obtained for the point electric source $D_3 = d\delta(x)$ C/m; $\delta(x)$ is Dirac delta-function. Both these characteristics give similar information about the ranges of individual mode domination or attenuation. And the use of Eq. (1) for the GW power estimation seems to be more advantageous as it directly yields the GW amplitudes accounting for the source parameters.

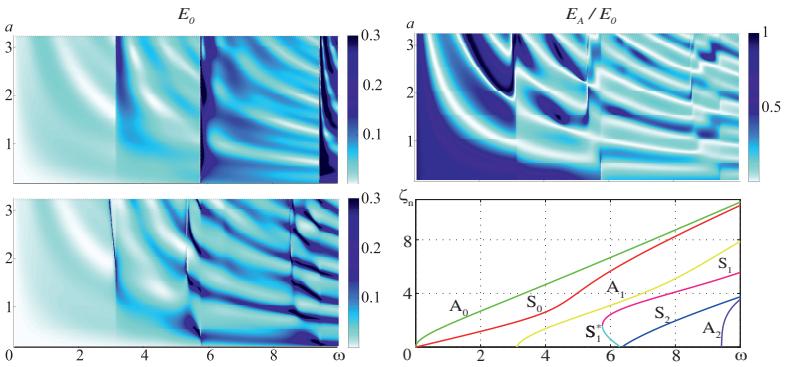

Fig. 4. Simulated within coupled (top) and uncoupled (bottom-left) models source energy E_0 and the part of A_0 energy E_A/E_0 as functions of ω and a; substracture's dispersion properties (bottom-right).

3. PWAS power distribution among the excited GWs

The active elements of SHM systems are often made of flexible piezoelectric patches that are bonded to the inspected structure (Fig. 1b). The longitudinal patch deformation caused by a driving electric field E_z due to piezoelectric effect results in a shear contact traction $\tau_{xz} = q(x)$ at the patch-structure interface. The traction q applied to the substructure generates traveling elastic waves described by the GW expansion in Eq. (1). The source (PWAS) controls the GW amplitudes via the traction's Fourier symbol $Q(\alpha) = \mathcal{F}_x[q]$ in Eq. (2). In general, $q(x)$ is unknown and has to be obtained from a coupled contact problem accounting for both patch and plate deformation under the bonding condition in the contact area $|x| \le a$.

In widely used simplified uncoupled models the PWAS action is approximated by two oppositely directed tangential point forces applied at the patch edges: $q(x) = q_0[\delta(x-a) - \delta(x+a)]$; Giurgiutiu (2000). It yields reasonably good results at low frequencies. However, they become worse with increasing frequency, especially when higher Lamb modes appear in addition to the fundamental symmetric and antisymmetric modes S_0 and A_0. To improve the results, the contact problem arising in the coupled model has been brought to the Wiener-Hopf type integral equation and solved via reducing it to a stably truncated infinite algebraic system; Glushkov et al. (2007). As an example, Fig. 4 depicts the time-averaged energy E_0 supplied by PWAS and the part of the A_0 mode energy E_A in the total source power E_0 obtained as functions of frequency ω and patch semi-width a within the coupled and uncoupled models.

Acknowledgements

The work is supported by the Russian Foundation for Basic Research together with the Administration of Krasnodar Region (project No. 13-01-96520) and by the Russian Ministry of Science and Education (project No. 1.189.2014K).

References

Nakahata, H., Higaki, K., Fujii, S., Hachigo, A., Kitabayashi, H.,Tanabe, K., Seki, Y., Shikata, S., 1995. SAW Devices on Diamond, Proceedings of IEEE Ultrasonics Symposium, Seattle, WA, USA, 7-10 Nov. V. 1, 361-370.

Benetti, M., Cannatà, D., Di Pietrantonio, F., Fedosov, V.I., Verona, E., 2005. Growth of A1N piezoelectric film on diamond for high-frequency surface acoustic wave devices, IEEE Ultrasonics Symposium, 1868.

Wu, S., Ro, R., Lin, Z. X., Lee, M. S., 2008. Rayleigh surface acoustic wave modes of interdigital transducer/(100) AlN/(111) diamond. J. Appl. Phys. 104, 064919.

Glushkov,E., Glushkova, N., Zhang, C., 2012. Surface and pseudo-surface acoustic waves piezoelectically excited in diamond-based structures. J. Appl. Phys. 112, 064911.

Giurgiutiu, V., Zagrai, A., 2000. Characterization of piezoelectric wafer active sensors. J. Intell. Mater. Syst. Struct. 11, 959-975.

Glushkov, E., Glushkova, N., Kvasha O., Seemann, W., 2007. Integral equation based modeling of the interaction between piezoelectric patch actuators and an elastic substrate. Smart Mater. Struct. 16, 650-664.